

Solving Combinatorial Pricing Problems using Embedded Dynamic Programming Models

Quang Minh Bui¹, Margarida Carvalho¹, and José Neto²

¹CIRRELT and Département d'informatique et de recherche opérationnelle, Université de Montréal

²Télécom SudParis, Institut Polytechnique de Paris

Abstract

The combinatorial pricing problem (CPP) is a bilevel problem in which the leader maximizes their revenue by imposing tolls on certain items that they can control. Based on the tolls set by the leader, the follower selects a subset of items corresponding to an optimal solution of a combinatorial optimization problem. To accomplish the leader's goal, the tolls need to be sufficiently low to discourage the follower from choosing the items offered by the competitors. In this paper, we derive a single-level reformulation for the CPP by rewriting the follower's problem as a longest path problem using a dynamic programming model, and then taking its dual and applying strong duality. We proceed to solve the reformulation in a dynamic fashion with a cutting plane method. We apply this methodology to 2 distinct dynamic programming models, namely, a novel formulation designated as selection diagram and the well-known decision diagram. We also produce numerical results to evaluate their performances across 3 different specializations of the CPP and a closely related problem that is the knapsack interdiction problem. Our results showcase the potential of the 2 proposed reformulations over the natural value function approach, expanding the set of tools to solve combinatorial bilevel programs.

1 Introduction

Consider a bilevel problem with 2 decision makers where one agent, the *leader*, sets the *tolls* (*i.e.* markups) of certain items, then the other agent, the *follower*, selects a subset of items according to another optimization problem (also known as the *follower's problem*). The follower has a choice between the items that the leader controls (called *tolled items*), and other items offered by the leader's competitors, whose prices, we assume, are fixed. The goal of the leader is to maximize the sum of tolls of the selected tolled items. Although the leader naturally wants to set the tolls high, such tolls cannot be excessive since the leader still needs the follower to choose their items in order to gain a profit. Thus,

the objectives of the 2 agents are neither adversarial nor cooperative. In this paper, we investigate the case where the follower’s problem is a combinatorial optimization problem which can be expressed as a binary linear program. We refer to the overall bilevel problem as *combinatorial pricing problem* (CPP). In the literature, the CPP is also called the Stackelberg pricing game.

Motivation The CPP is inspired by the network pricing problem (NPP) introduced by Labbé et al. [21]. The NPP is a specific case of the CPP where the follower’s problem is a shortest path problem. In the CPP, the shortest path problem is replaced by other combinatorial problems such as the minimum spanning tree problem [10], the knapsack problem [4, 24], the stable set problem [8], and the bipartite vertex cover problem [5]. This class of problems is usually proven to be NP-hard [10, 25] or even Σ_2^P -hard [8].

Except for the NPP, most papers in the literature focus on the problems computational complexity classification and approximation schemes. Regarding the exact solution methods, general bilevel solvers like MibS [26] or the one by Fischetti et al. [15] are not applicable due to the leader’s variables (the tolls in this case) being continuous and not appearing in the follower’s constraints. A popular method to solve the NPP is to find a dual of the follower’s problem and then use the Karush-Kuhn-Tucker conditions to convert the bilevel problem to a single-level reformulation [3, 7, 14, 20]. This method, referred to as *dualize-and-combine*, is not trivial to generalize to the CPP because a dual of a binary linear program is not generally defined and even if it exists, it is often computationally untractable. A relatively novel technique to formulate a dual is described in Lozano et al. [22], in which the authors use decision diagrams [1] to derive single-level reformulations for (bilevel) interdiction problems. This approach requires the assumption that the decision diagram model is of computationally tractable size allowing to apply off-the-shelf solvers directly to their reformulation.

Contributions Our first contribution is the application of the technique in Lozano et al. [22] to the CPP. We convert the follower’s problem into an equivalent longest path problem corresponding to a dynamic programming model. The longest path problem has a linear programming formulation, hence we can dualize this linear program and combine it with the original primal follower’s program to create a valid single-level reformulation for the CPP. Besides decision diagrams, we also propose and evaluate a new dynamic programming model called *selection diagram*.

Even with the reformulation well-defined, the computational untractability issue still remains due to the very likely large size of the reformulation. Thus, our second contribution is the proposition of a dynamic constraint generation scheme similar to the cutting plane method. Notably, we describe methodologies to generate initial selection and decision diagrams, to add follower’s solutions to them, and to avoid the increase on the number of layers of the decision diagrams.

Our third contribution is the numerical results comparing the performance of these formulations in the context of 3 specializations of the CPP, in which the

follower’s problems are the knapsack problem, the maximum stable set problem, and the minimum set cover problem, respectively. We also apply the same methodology to the knapsack interdiction problem, which can be reformulated as a special case of the CPP. These results support a promising direction to scale the solving of the CPP.

Paper Organization In [Section 2](#), we describe the bilevel formulation of the CPP and its *value function reformulation*, which serves as an introduction to the dualize-and-combine methodology. We define 2 different dynamic programming models: selection diagram and decision diagram in [Section 3](#), as well as the dynamic constraint generation algorithms corresponding to each model. [Section 4](#) presents the experimental setups and numerical results. Finally, [Section 5](#) concludes the paper.

2 Combinatorial Pricing Problem

2.1 Problem Description

Consider a combinatorial optimization problem with decision variables $x \in \mathcal{X} \subseteq \{0, 1\}^{\mathcal{I}}$ indexed by the set of *items* \mathcal{I} . Each item $i \in \mathcal{I}$ has an associated *base value* $v_i \in \mathbb{R}$. The set \mathcal{I} is partitioned into the set of *tolled items* \mathcal{I}_1 and the set of *toll-free items* \mathcal{I}_2 . The leader wishes to impose a toll $t_i \geq 0$ for each tolled item $i \in \mathcal{I}_1$. For the toll-free items $i \in \mathcal{I}_2$, we set $t_i = 0$. Let $\mathcal{T} = \mathbb{R}_+^{\mathcal{I}_1} \times \{0\}^{\mathcal{I}_2}$ be the set of feasible tolls. The overall CPP is formulated as a bilevel program:

$$\max_{t,x} \{t^\top x \mid t \in \mathcal{T}, x \in \mathbf{R}(t)\}$$

where $\mathbf{R}(t) \subseteq \mathcal{X}$ is the set of optimal solutions of the *follower’s problem* given the toll t , defined by:

$$\mathbf{R}(t) = \arg \max_x \{(v - t)^\top x \mid x \in \mathcal{X}\}. \quad (1)$$

Note that if $\mathbf{R}(t)$ is not a singleton, *i.e.* there are multiple optimal solutions of the follower’s problem, then the follower will choose a solution x that yields the most revenue $t^\top x$ for the leader. This is commonly referred to as the *optimistic assumption*.

Example 1. The *knapsack pricing problem* (KPP) is a case of the CPP where the underlying optimization problem is a knapsack problem. Let $w \in \mathbb{R}_+^{\mathcal{I}}$ and $C > 0$ be the knapsack weights and capacity, respectively. Then, the follower’s problem of the KPP becomes:

$$\mathbf{R}(t) = \arg \max_x \{(v - t)^\top x \mid w^\top x \leq C, x \in \{0, 1\}^{\mathcal{I}}\}.$$

We make several remarks regarding the KPP:

Remark 1. The leader has no incentive to set $t_i > v_i$. Indeed, in the perspective of the follower, $v_i - t_i < 0$ is the same as $v_i - t_i = 0$, and neither case gives the leader any revenue, so the leader may as well set $t_i = v_i$. Thus, we can assume that $t_i \leq v_i$ for all $i \in \mathcal{I}$.

Remark 2. There always exists an optimal solution x^* of the KPP that is maximal. This follows [Remark 1](#), since including any new item produces a profit for both the follower and the leader. This property is referred to as *monotonicity* [17].

2.2 Value Function Formulation

One method to solve the CPP is to convert the bilevel program into a single-level reformulation. Such formulation requires a dual representation of the follower's problem (1). The follower's problems that we are interested in are binary programs, hence the dual representation is not trivial to derive. Despite that, next we show how such dual representation could be determined and used within a cutting plane method.

Define a new binary variable $z_{\hat{x}} \in \{0, 1\}$ that indicates if a particular solution $\hat{x} \in \mathcal{X}$ is selected or not. We reformulate [Program \(1\)](#) as follows:

$$\max_z \left\{ \sum_{\hat{x} \in \mathcal{X}} ((v - t)^\top \hat{x}) z_{\hat{x}} \mid \sum_{\hat{x} \in \mathcal{X}} z_{\hat{x}} = 1, z \in \{0, 1\}^{\mathcal{X}} \right\}. \quad (2)$$

[Program \(2\)](#) is totally unimodular, hence we can relax $z \in \{0, 1\}^{\mathcal{X}}$ to $z \geq 0$. The dual of its linear relaxation is:

$$\min_L \{L \mid L \geq (v - t)^\top \hat{x}, \hat{x} \in \mathcal{X}\}. \quad (3)$$

Combining [Program \(1\)](#) and [Program \(3\)](#) with the strong duality condition, we derive the single-level reformulation:

$$\max_{t, x, L} t^\top x \quad (4a)$$

$$\text{s.t. } x \in \mathcal{X}, \quad (4b)$$

$$L \geq (v - t)^\top \hat{x}, \quad \hat{x} \in \mathcal{X}, \quad (4c)$$

$$(v - t)^\top x = L, \quad (4d)$$

$$t \in \mathcal{T}. \quad (4e)$$

Observe that [Constraints \(4c\)](#) and [\(4d\)](#) imply:

$$(v - t)^\top x \geq (v - t)^\top \hat{x}, \quad \hat{x} \in \mathcal{X}. \quad (5)$$

This is usually referred as the *(optimal) value function constraint*. Thus, we refer to [Program \(4\)](#) as the *value function formulation*.

Example 2. Consider a KPP instance of 4 items $\mathcal{I} = \{1, 2, 3, 4\}$. The first 3 items are tolled, *i.e.* $\mathcal{I}_1 = \{1, 2, 3\}$, and $\mathcal{I}_2 = \{4\}$. The base values are $v = (1, 1, 1, 1)$. The knapsack weights and capacity are $w = (1, 1, 1, 2)$ and $C = 3$ respectively. Thus, we have

$$\mathcal{X} = \{x \in \{0, 1\}^4 \mid x_1 + x_2 + x_3 + 2x_4 \leq 3\}.$$

By [Remark 2](#), we only need to keep track of the maximal solutions. There are 4 maximal solutions in \mathcal{X} : $(1, 1, 1, 0)$, $(1, 0, 0, 1)$, $(0, 1, 0, 1)$, and $(0, 0, 1, 1)$. It is more convenient to refer to them as the sets they represent: $\{1, 2, 3\}$, $\{1, 4\}$, $\{2, 4\}$, and $\{3, 4\}$. The value function formulation corresponding to this KPP instance is:

$$\begin{aligned} \max_{t, x, L} \quad & t_1 x_1 + t_2 x_2 + t_3 x_3 \\ \text{s.t.} \quad & x_1 + x_2 + x_3 + 2x_4 \leq 3, \\ & L \geq 3 - t_1 - t_2 - t_3, \\ & L \geq 2 - t_1, \\ & L \geq 2 - t_2, \\ & L \geq 2 - t_3, \\ & (1 - t_1)x_1 + (1 - t_2)x_2 + (1 - t_3)x_3 + x_4 = L, \\ & x \in \{0, 1\}^4, \\ & t \geq 0. \end{aligned}$$

To solve [Program \(4\)](#) as a mixed-integer linear program (MILP), we need to linearize the bilinear terms $t^\top x$. This can be done using the McCormick envelope [\[23\]](#) by replacing $t_i x_i$ for each $i \in \mathcal{I}_1$ with s_i , accompanied by the following constraints:

$$0 \leq s_i \leq M_i x_i, \quad 0 \leq t_i - s_i \leq M_i(1 - x_i), \quad (6)$$

where M_i is a sufficiently large bound of $t_i x_i$. For instance, a valid bound for the KPP is $M_i = v_i$ due to [Remark 1](#).

Typically, the size of \mathcal{X} is exponential, so in practice, we generate [Constraint \(4c\)](#) dynamically in a cutting plane fashion as described in [Algorithm 1](#).

3 Embedded Dynamic Programming Model

The value function formulation in [Program \(4\)](#) is simple and general. However, the structure of the follower's problem is oblivious to the dual representation. We aim to introduce some structural information back to the dual in the form of a dynamic programming (DP) model. It is well-known that any DP model with a finite number of states and actions can be represented as a directed multigraph [\[2\]](#). Thus, for our convenience, we define all DP models by their graph representations. Suppose that the follower's problem possesses a DP model whose definition includes:

Algorithm 1 Solution of [Program \(4\)](#) with dynamically generated constraints

Input: The CPP instance.

Output: The optimal solution (t^*, x^*) of the CPP instance.

```

1: Create the master problem from Program \(4\) without Constraint \(4c\).
2: loop
3:   Solve the master problem and let  $(\tilde{t}, \tilde{x})$  be the current optimal solution.
4:   Solve Program \(1\) with  $t = \tilde{t}$  for  $\hat{x}$ . ▷ i.e. choose any  $\hat{x} \in \mathbf{R}(\tilde{t})$ 
5:   if  $(v - \tilde{t})^\top \tilde{x} < (v - \tilde{t})^\top \hat{x}$  then
6:     ▷  $(\tilde{t}, \tilde{x})$  is not bilevel feasible. Add new constraint. ◁
7:     Add the constraint  $L \geq (v - \tilde{t})^\top \hat{x}$  to the master program.
8:   else
9:     ▷  $(\tilde{t}, \tilde{x})$  is bilevel feasible. Stop. ◁
10:     $(t^*, x^*) \leftarrow (\tilde{t}, \tilde{x})$ 
11:  break
12: return  $(t^*, x^*)$ 

```

- A set of *nodes* \mathcal{V} (corresponding to the *states*);
- A set of *arcs* \mathcal{A} (corresponding to the *actions*);
- Two functions $u, w : \mathcal{A} \rightarrow \mathcal{V}$ that return the source node $u(a)$ and the target node $w(a)$ of arc a , respectively;
- An *item function* $I : \mathcal{A} \rightarrow 2^{\mathcal{I}}$ which is later used to define the length of the arcs;
- An *initial node* $p \in \mathcal{V}$ and a *terminal node* $q \in \mathcal{V}$.

The directed multigraph $(\mathcal{V}, \mathcal{A}, u, w)$ must be acyclic. We define the *length* $F(a; t)$ of arc $a \in \mathcal{A}$ given toll $t \in \mathcal{T}$ as the sum of the tolled values of all the items in $I(a)$:

$$F(a; t) = \sum_{i \in I(a)} (v_i - t_i).$$

The objective of the DP model is to find the longest path from p to q . Henceforth, when we refer to *paths*, we mean paths from p to q . This optimization problem can be expressed by the following formulation (which is the dual of a typical linear formulation for the longest path problem):

$$\min_y y_p \tag{7a}$$

$$\text{s.t. } y_{u(a)} \geq F(a; t) + y_{w(a)}, \quad a \in \mathcal{A}, \tag{7b}$$

$$y_q = 0. \tag{7c}$$

Because the DP model is equivalent to the follower's problem (*i.e.* they return the same optimal objective value), we can use [Program \(7\)](#) as a dual

representation in a similar way to [Program \(3\)](#). The result is a new single-level reformulation¹:

$$\max_{t,x,y} t^\top x \tag{8a}$$

$$\text{s.t. } x \in \mathcal{X}, \tag{8b}$$

$$y_{u(a)} \geq F(a; t) + y_{w(a)}, \quad a \in \mathcal{A}, \tag{8c}$$

$$y_q = 0, \tag{8d}$$

$$(v - t)^\top x = y_p, \tag{8e}$$

$$t \in \mathcal{T}. \tag{8f}$$

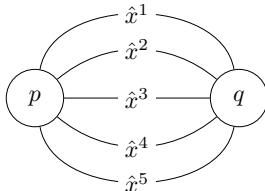


Figure 1: Value function formulation as a DP model.

Example 3. The value function formulation [Program \(4\)](#) can be thought as a special case of [Program \(8\)](#). Indeed, consider a DP model consisting of only 2 nodes p and q . Each solution $\hat{x} \in \mathcal{X}$ corresponds to an arc $a_{\hat{x}} \in \mathcal{A}$. The item function is defined to be the set of items selected in \hat{x} :

$$I(a_{\hat{x}}) = \{i \in \mathcal{I} \mid \hat{x}_i = 1\}.$$

Then, the variable L in [Program \(4\)](#) is identical to y_p in [Program \(8\)](#). The DP graph of the value function formulation is shown in [Figure 1](#). In all graphs illustrated in this paper, the arcs are always directed from left to right.

Next, we explore the application of [Program \(8\)](#) to 2 types of DP models: *selection diagrams* ([Section 3.1](#)) and *decision diagrams* ([Section 3.2](#)). The former defines the actions based on the items to be selected, while the latter defines the actions as decisions to include or exclude a specific item. For each type of model, we also describe the procedure to solve [Program \(8\)](#) dynamically as in [Algorithm 1](#) alongside any other technical improvement.

3.1 Selection Diagram

The first family of dynamic programming models that we investigate is called *selection diagram*. In a selection diagram, at each step, the follower either selects

¹[\[22\]](#) obtain a similar single-level reformulation. However, [Program \(8\)](#) uses the follower's original representation of the feasible region, [Constraint \(8b\)](#), while [\[22\]](#) uses the path formulation resulting from the DP model.

an item to be included into the current partial solution, or decides to stop and returns the solution. In particular, let $\mathcal{I}(\hat{x}) = \{i \in \mathcal{I} \mid \hat{x}_i = 1\}$ be the set of items selected in $\hat{x} \in \mathcal{X}$. The set of nodes in a selection diagram is the family of subsets of \mathcal{I} that are contained in some feasible solution in \mathcal{X} , adjoined with a special terminal node q :

$$\mathcal{V} = \{J \subseteq \mathcal{I} \mid J \subseteq \mathcal{I}(\hat{x}) \text{ for some } \hat{x} \in \mathcal{X}\} \cup \{q\}.$$

The initial node p in this case is the node \emptyset .

For every pair of nonterminal nodes $J, K \in \mathcal{V} \setminus \{q\}$ such that $J \subseteq K$ and $|K| - |J| = 1$, we add an arc a_{JK} from J to K such that $I(a_{JK}) = K \setminus J$. Evidently, $I(a_{JK})$ is a singleton. Moreover, given a nonterminal node J , if $J = \mathcal{I}(\hat{x})$ for some $\hat{x} \in \mathcal{X}$, then we connect J directly to q with a *terminal arc* \bar{a}_J with $I(\bar{a}_J) = \emptyset$.

With this construction, the nodes on a path from \emptyset to q form a sequence of nested subsets of \mathcal{I} :

$$\emptyset, \{i_1\}, \{i_1, i_2\}, \dots, \{i_1, \dots, i_n\}, q$$

such that $\{i_1, \dots, i_n\} = \mathcal{I}(\hat{x})$ for some $\hat{x} \in \mathcal{X}$. The length of such a path is exactly $(v - t)^\top \hat{x}$. Thus, finding the longest path in a selection diagram is equivalent to finding the solution $\hat{x} \in \mathcal{X}$ that yields the highest objective value for the follower.

Example 4. The selection diagram for the KPP instance in [Example 2](#) is illustrated in [Figure 2](#). Once again, we only keep track of the 4 maximal solutions: $\{1, 2, 3\}$, $\{1, 4\}$, $\{2, 4\}$, $\{3, 4\}$. Note that a given solution $\hat{x} \in \mathcal{X}$ may be represented by multiple paths from \emptyset to q . Applying [Program \(8\)](#) to [Figure 2](#), [Constraints \(8c\)](#) and [\(8d\)](#) become:

$$\begin{aligned} y_\emptyset &\geq 1 - t_1 + y_1, & y_\emptyset &\geq 1 - t_2 + y_2, & y_\emptyset &\geq 1 - t_3 + y_3, & y_\emptyset &\geq 1 + y_4, \\ y_1 &\geq 1 - t_2 + y_{12}, & y_2 &\geq 1 - t_1 + y_{12}, & y_3 &\geq 1 - t_1 + y_{13}, & y_4 &\geq 1 - t_1 + y_{14}, \\ y_1 &\geq 1 - t_3 + y_{13}, & y_2 &\geq 1 - t_3 + y_{23}, & y_3 &\geq 1 - t_2 + y_{23}, & y_4 &\geq 1 - t_2 + y_{24}, \\ y_1 &\geq 1 + y_{14}, & y_2 &\geq 1 + y_{24}, & y_3 &\geq 1 + y_{34}, & y_4 &\geq 1 - t_3 + y_{34}, \\ y_{12} &\geq 1 - t_3 + y_{123}, & y_{13} &\geq 1 - t_2 + y_{123}, & y_{23} &\geq 1 - t_1 + y_{123}, & & \\ y_{14} &\geq 0, & y_{24} &\geq 0, & y_{34} &\geq 0, & y_{123} &\geq 0. \end{aligned}$$

3.1.1 Dynamic Generation

The number of subsets of \mathcal{I} is exponential with respect to $|\mathcal{I}|$, so in practice, enumerating the full set of [Constraints \(8c\)](#) and [\(8d\)](#), as in [Example 4](#), is untractable. Thus, a method to generate the variables and constraints dynamically is required. Furthermore, some popular MILP solvers do not support column generation, so the dynamic generation of the variables y_J is usually not feasible. In this section, we describe an algorithm to solve [Program \(8\)](#) using a selection diagram which is updated dynamically only with new constraints (which are often referred to as *lazy constraints*).

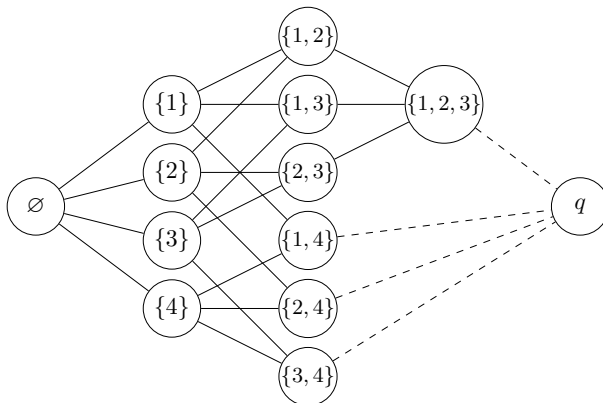


Figure 2: Selection diagram of [Example 4](#). Dashed arcs represent the terminal arcs.

The first step is to choose a set of nodes $\hat{\mathcal{V}}$ that will be used throughout the procedure. This set of nodes is final, since we do not opt for column generation. Evidently, the initial node \emptyset and the terminal node q must be in $\hat{\mathcal{V}}$. For the remaining nodes, we limit our options to only singletons and pairs, *i.e.* we only consider the nodes J where $|J| \in \{1, 2\}$. Even so, some pairs may not belong to a feasible solution, and the number of all pairs is often too large, hence not every pair should be present in the selection diagram. We propose a sampling algorithm described in [Algorithm 2](#). The algorithm iteratively samples a solution $\hat{x} \in \mathcal{X}$, then it randomly selects a pair within $\mathcal{I}(\hat{x})$. After reaching the desired number of pairs, it builds the connections within the first 2 layers. The end result is an initial selection diagram to be used in [Program \(8\)](#).

The single-level reformulation ([Program \(8\)](#)) derived from the initial selection diagram is a relaxation of the one derived from the full selection diagram. Indeed, we did not connect any node to the terminal node q . As a result, the value of y_\emptyset is not “grounded” and the dual representation has no effect at the beginning. Over the course of the procedure, we introduce new paths by connecting nonterminal nodes J to q using a *modified terminal arc* \hat{a}_J . As long as the paths that we add to the diagram correspond to feasible solutions in \mathcal{X} , the reformulation remains valid. Such solutions are obtained by solving the follower’s problem similarly to [Algorithm 1](#). The whole process is described in [Algorithm 3](#).

Example 5. Consider the KPP instance introduced in [Example 2](#). At line 4 in [Algorithm 2](#), instead of sampling a random solution, we once again exploit monotonicity ([Remark 2](#)) and sample only maximal solutions in \mathcal{X} . Suppose that we sample the 2 pairs $\{1, 2\}$ and $\{2, 4\}$ in line 5. The initial selection diagram returned by [Algorithm 2](#) is drawn in [Figure 3](#) (consider only the solid arcs).

The dashed arcs in [Figure 3](#) represent the modified terminal arcs added by

Algorithm 2 Generation of the initial selection diagram

Input: The CPP instance, the desired number of pairs N .**Output:** The set of nodes $\hat{\mathcal{V}}$ and the set of initial arcs $\hat{\mathcal{A}}$.

```
1:  $\triangleright$  Initial nodes  $\triangleleft$ 
2:  $\hat{\mathcal{V}}_0 \leftarrow \{\emptyset\}, \hat{\mathcal{V}}_1 \leftarrow \emptyset, \hat{\mathcal{V}}_2 \leftarrow \emptyset$ 
3: for  $n = 1, \dots, N$  do
4:   Sample  $\hat{x} \in \mathcal{X}$ 
5:   Sample a random pair  $\{i, j\}$  within  $\mathcal{I}(\hat{x})$ 
6:    $\hat{\mathcal{V}}_1 \leftarrow \hat{\mathcal{V}}_1 \cup \{i, j\}$   $\triangleright$  Set of singletons
7:    $\hat{\mathcal{V}}_2 \leftarrow \hat{\mathcal{V}}_2 \cup \{\{i, j\}\}$   $\triangleright$  Set of pairs
8:  $\hat{\mathcal{V}} \leftarrow \hat{\mathcal{V}}_0 \cup \hat{\mathcal{V}}_1 \cup \hat{\mathcal{V}}_2 \cup \{q\}$ 
9:  $\triangleright$  Initial arcs  $\triangleleft$ 
10:  $\hat{\mathcal{A}} \leftarrow \emptyset$ 
11: for  $k = 1, 2$  do
12:   for all  $J \in \hat{\mathcal{V}}_{k-1}, K \in \hat{\mathcal{V}}_k$  do
13:     if  $J \subseteq K$  then
14:       Create an arc  $a_{JK}$  from  $J$  to  $K$ 
15:        $I(a_{JK}) \leftarrow K \setminus J$ 
16:        $\hat{\mathcal{A}} \leftarrow \hat{\mathcal{A}} \cup \{a_{JK}\}$ 
17: return  $(\hat{\mathcal{V}}, \hat{\mathcal{A}})$ 
```

Algorithm 3 corresponding to the 4 maximal solutions. The 2 solutions $\{1, 2, 3\}$ and $\{2, 4\}$ contain some pairs in the initial diagram, hence we can connect those pairs to q (which is the best case). There is no pair contained in the other 2 solutions $\{1, 4\}$ and $\{3, 4\}$, so we fall back to singletons. Note that some solutions like $\{1, 4\}$ can be introduced in multiple ways (from either state $\{1\}$ or $\{4\}$). In that case, we choose a random node by iterating $\hat{\mathcal{V}}_k$ in a random order (line 9 in **Algorithm 3**). In the worst case, we can add an arc from \emptyset directly to q , which is equivalent to a value function constraint. Thus, we can always introduce any feasible solution into the diagram.

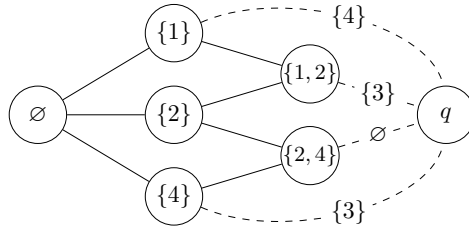


Figure 3: Dynamically generated selection diagram of **Example 5**. Solid arcs are the initial arcs, while dashed arcs represent the modified terminal arcs added during **Algorithm 3**. The labels of the dashed arcs are $I(\hat{a}_J)$.

Algorithm 3 Solution of [Program \(8\)](#) using selection diagram with dynamically generated constraints

Input: The CPP instance, the initial selection diagram $(\hat{\mathcal{V}}, \hat{\mathcal{A}})$.

Output: The optimal solution (t^*, x^*) of the CPP instance.

- 1: Create the master problem from [Program \(8\)](#) using the diagram $(\hat{\mathcal{V}}, \hat{\mathcal{A}})$.
- 2: **loop**
- 3: Solve the master problem and let (\tilde{t}, \tilde{x}) be the current optimal solution.
- 4: Solve [Program \(1\)](#) with $t = \tilde{t}$ for \hat{x} . \triangleright i.e. choose any $\hat{x} \in \mathbf{R}(\tilde{t})$
- 5: **if** $(v - \tilde{t})^\top \tilde{x} < (v - \tilde{t})^\top \hat{x}$ **then**
- 6: $\triangleright (\tilde{t}, \tilde{x})$ is not bilevel feasible. Add new constraint. \triangleleft
- 7: added \leftarrow **false**
- 8: **for** $k = 2, 1, 0$ **do**
- 9: **for all** $J \in \hat{\mathcal{V}}_k$ **do** \triangleright Iterate in a random order
- 10: **if** $J \subseteq \mathcal{I}(\hat{x})$ **then**
- 11: Create an arc \hat{a}_J from J to q
- 12: $I(\hat{a}_J) \leftarrow \mathcal{I}(\hat{x}) \setminus J$
- 13: $\hat{\mathcal{A}} \leftarrow \hat{\mathcal{A}} \cup \{\hat{a}_J\}$
- 14: Add $y_J \geq \sum_{i \in I(\hat{a}_J)} (v_i - t_i)$ to the master program.
- 15: added \leftarrow **true**
- 16: **break**
- 17: **if** added **then**
- 18: **break** \triangleright Break the loop, go back to the outer loop
- 19: **else**
- 20: $\triangleright (\tilde{t}, \tilde{x})$ is bilevel feasible. Stop. \triangleleft
- 21: $(t^*, x^*) \leftarrow (\tilde{t}, \tilde{x})$
- 22: **break**
- 23: **return** (t^*, x^*)

3.2 Decision Diagram

A family of dynamic programming models that is commonly used in the literature is *decision diagrams* [1, 22]. In a decision diagram, each step represents the decision to include or exclude a specific item. Let $n = |\mathcal{I}|$ and let (i_1, i_2, \dots, i_n) be an ordering of the items in \mathcal{I} . A *proper node* (neither p nor q) in a decision diagram is a tuple (k, s_k) of a step $k \in \{1, \dots, n-1\}$ and a state s_k . The definition of the states s_k is problem-specific. We partition \mathcal{V} into $n+1$ layers: \mathcal{V}_0 which contains only p ; \mathcal{V}_k which contains all nodes (k, s_k) for $k = 1, \dots, n-1$; and \mathcal{V}_n which contains only q .

For $k = 0, \dots, n-1$, a node $u_k \in \mathcal{V}_k$ has at most 2 outgoing arcs $a_{u_k}^0$ and $a_{u_k}^1$, corresponding to the decisions $x_{i_{k+1}} = 0$ and $x_{i_{k+1}} = 1$. The targets of these arcs are in the next layer \mathcal{V}_{k+1} . The item function is defined as follows:

$$I(a_{u_k}^0) = \emptyset, \quad I(a_{u_k}^1) = \{i_{k+1}\}.$$

A path in a decision diagram represents a series of decisions $(x_{i_1}, \dots, x_{i_n})$, fixing the choice of one item at every step. At the end of the path, all entries

in x have been fixed and the value of x should correspond to a feasible solution $\hat{x} \in \mathcal{X}$ given a suitable description of the nodes. In this paper, we provide the descriptions of the decision diagrams for 3 specific problems: the knapsack problem (Example 6), the maximum stable set problem (Section 3.2.3), and the minimum set cover problem (Section 3.2.4). The descriptions of the decision diagrams for several other problems can be found in [1].

Example 6. In the decision diagram of the knapsack problem, we define the state s_k at step k as the remaining capacity after x_{i_1}, \dots, x_{i_k} have been decided. Furthermore, we express the initial node p as $(0, C)$ and the terminal node q as $(n, 0)$. The arc $a_{u_k}^0$ is always available and it sends (k, s_k) to $(k+1, s_k)$. The arc $a_{u_k}^1$ only exists if $s_k \geq w_{i_{k+1}}$, *i.e.* there is enough remaining capacity to fit the item i_{k+1} . In that case, it connects (k, s_k) to $(k+1, s_k - w_{i_{k+1}})$. An exception is that all arcs from the second-to-last layer \mathcal{V}_{n-1} end at the terminal node instead.

The decision diagram for the KPP instance in Example 2 is illustrated in Figure 4a. We can use Remark 2 to simplify the graph. At step k , if the state s_k satisfies $s_k \geq \sum_{j=k+1}^n w_{i_j}$, then we must set $x_{i_j} = 1$ for all $j > k$ in order to have a maximal solution. Thus, for each k , we can merge all states s_k such that $s_k \geq \sum_{j=k+1}^n w_{i_j}$. Furthermore, if $a_{u_k}^0$ and $a_{u_k}^1$ end at the same node, we can eliminate $a_{u_k}^0$ since including the item i_k is prioritized. The final result is shown in Figure 4b. Applying Program (8) to Figure 4b, Constraints (8c) and (8d) become (note that $y_p = y_{0,3}$):

$$\begin{aligned}
y_{0,3} &\geq y_{1,3}, & y_{0,3} &\geq 1 - t_1 + y_{1,2}, & y_{2,1} &\geq y_{3,1}, & y_{2,1} &\geq 1 - t_3 + y_{3,0}, \\
y_{1,2} &\geq y_{2,2}, & y_{1,2} &\geq 1 - t_2 + y_{2,1}, & y_{2,2} &\geq y_{3,2}, & y_{2,2} &\geq 1 - t_3 + y_{3,1}, \\
y_{1,3} &\geq y_{2,3}, & y_{1,3} &\geq 1 - t_2 + y_{2,2}, & y_{3,0} &\geq 0, & y_{2,3} &\geq 1 - t_3 + y_{3,2}, \\
&&&&&&& y_{3,1} &\geq 0, & y_{3,2} &\geq 1.
\end{aligned}$$

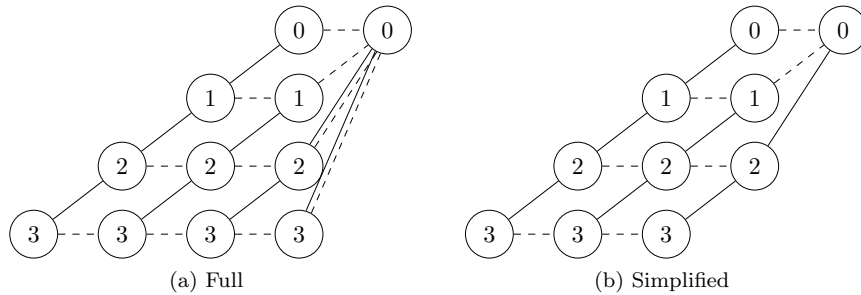


Figure 4: Decision diagrams of Example 6. The labels of the nodes are the states s_k . The steps of the nodes are implied from left to right as $k = 0, \dots, 4$. Solid arcs and dashed arcs represent the decisions $x_k = 1$ and $x_k = 0$, respectively.

3.2.1 Dynamic Generation

Similar to selection diagrams, the number of nodes in a decision diagram is exponential on $|\mathcal{I}|$. Thus, we also wish to solve [Program \(8\)](#) using a dynamically generated decision diagram. [Algorithm 4](#) describes a sampling algorithm that returns an initial decision diagram. The size of the initial decision diagram is controlled by a parameter W which is called the *width* of the diagram. As the name suggests, it holds that $|\hat{\mathcal{V}}_k| \leq W$ for all $k = 1, \dots, n-1$. The algorithm samples exactly W solutions $\hat{x} \in \mathcal{X}$ (line 4), finds a path in the full diagram for each \hat{x} (line 5), then incorporates those paths into the initial diagram (lines 6 and 7). The path-finding step is problem-specific, but usually, it can be done quite efficiently without explicitly enumerating the full diagram.

Algorithm 4 Generation of the initial decision diagram

Input: The CPP instance, the desired width W .

Output: The set of nodes $\hat{\mathcal{V}}$ and the set of initial arcs $\hat{\mathcal{A}}$.

```

1:  $\hat{\mathcal{V}} \leftarrow \emptyset$   $\triangleright$  Initial nodes
2:  $\hat{\mathcal{A}} \leftarrow \emptyset$   $\triangleright$  Initial arcs
3: for  $\omega = 1, \dots, W$  do
4:   Sample  $\hat{x} \in \mathcal{X}$ 
5:   Find a path  $\pi$  corresponding to  $\hat{x}$  in the full decision diagram
6:    $\hat{\mathcal{V}} \leftarrow \hat{\mathcal{V}} \cup \mathcal{V}(\pi)$   $\triangleright \mathcal{V}(\pi)$  is the set of nodes in  $\pi$ 
7:    $\hat{\mathcal{A}} \leftarrow \hat{\mathcal{A}} \cup \mathcal{A}(\pi)$   $\triangleright \mathcal{A}(\pi)$  is the set of arcs in  $\pi$ 
8: return  $(\hat{\mathcal{V}}, \hat{\mathcal{A}})$ 

```

Updating a decision diagram is more complex than updating a selection diagram. We propose a method to append a path corresponding to a new solution $\hat{x} \in \mathcal{X}$ using as many nodes in $\hat{\mathcal{V}}$ as possible. Let \mathcal{B} be a superset of \mathcal{A} consisting of all *valid transitions* of the decision diagram, which is problem-specific. The longest path in $(\mathcal{V}, \mathcal{B})$ must have the same length as the longest path in $(\mathcal{V}, \mathcal{A})$. Unlike \mathcal{A} , for $b \in \mathcal{B}$, $u(b)$ and $w(b)$ need not be in consecutive layers, and $I(b)$ can have more than 1 item. For instance, \mathcal{B} can include, but is not limited to, the aggregations of path segments in \mathcal{A} . The testing of membership in \mathcal{B} should be fast and should not require the enumeration of \mathcal{B} .

We partition $\hat{\mathcal{V}}$ into layers $\hat{\mathcal{V}}_0, \dots, \hat{\mathcal{V}}_n$ such that $\hat{\mathcal{V}}_k \subseteq \mathcal{V}_k$ for all $k = 0, \dots, n$. Given a solution $\hat{x} \in \mathcal{X}$ that we wish to introduce into the diagram, consider the subset:

$$\hat{\mathcal{B}}(\hat{x}) = \{b \in \mathcal{B} \mid u(b) \in \hat{\mathcal{V}}_j, w(b) \in \hat{\mathcal{V}}_k, I(b) = \mathcal{I}_{jk}(\hat{x}) \text{ for some } j < k\}$$

where

$$\mathcal{I}_{jk}(\hat{x}) = \mathcal{I}(\hat{x}) \cap \{i_{j+1}, \dots, i_k\}.$$

Enumerating $\hat{\mathcal{B}}(\hat{x})$ takes $\mathcal{O}(|\hat{\mathcal{V}}|^2)$ -time assuming that the testing of membership in \mathcal{B} takes constant time (a loop for $u(b) \in \hat{\mathcal{V}}_j$ and an inner loop for $w(b) \in \hat{\mathcal{V}}_k$). By construction, every path in the graph $(\hat{\mathcal{V}}, \hat{\mathcal{B}}(\hat{x}))$ corresponds

to \hat{x} . We then find the longest path in $(\hat{\mathcal{V}}, \hat{\mathcal{B}}(\hat{x}))$ where the length of all arcs is exactly 1. Finally, we introduce this path as a set of new constraints. The whole process is outlined in [Algorithm 5](#).

Algorithm 5 Solution of [Program \(8\)](#) using decision diagram with dynamically generated constraints

Input: The CPP instance, the initial decision diagram $(\hat{\mathcal{V}}, \hat{\mathcal{A}})$.

Output: The optimal solution (t^*, x^*) of the CPP instance.

- 1: Create the master problem from [Program \(8\)](#) using the diagram $(\hat{\mathcal{V}}, \hat{\mathcal{A}})$.
- 2: **loop**
- 3: Solve the master problem and let (\tilde{t}, \tilde{x}) be the current optimal solution.
- 4: Solve [Program \(1\)](#) with $t = \tilde{t}$ for \hat{x} . \triangleright i.e. choose any $\hat{x} \in \mathbf{R}(\tilde{t})$
- 5: **if** $(v - \tilde{t})^\top \tilde{x} < (v - \tilde{t})^\top \hat{x}$ **then**
- 6: $\triangleright (\tilde{t}, \tilde{x})$ is not bilevel feasible. Add new constraint. \triangleleft
- 7: Enumerate $\hat{\mathcal{B}}(\hat{x})$.
- 8: Find the longest path π in $(\hat{\mathcal{V}}, \hat{\mathcal{B}}(\hat{x}))$ where all arcs have length 1.
- 9: $\hat{\mathcal{A}} \leftarrow \hat{\mathcal{A}} \cup \mathcal{A}(\pi)$ $\triangleright \mathcal{A}(\pi)$ is the set of arcs in π
- 10: **for** $a \in \mathcal{A}(\pi)$ **do**
- 11: Add $y_{u(a)} \geq \sum_{i \in I(a)} (v_i - t_i) + y_{w(a)}$ to the master program.
- 12: **else**
- 13: $\triangleright (\tilde{t}, \tilde{x})$ is bilevel feasible. Stop. \triangleleft
- 14: $(t^*, x^*) \leftarrow (\tilde{t}, \tilde{x})$
- 15: **break**
- 16: **return** (t^*, x^*)

Example 7. In the KPP, we can derive a path corresponding to a given $\hat{x} \in \mathcal{X}$ in the full diagram (line 5 in [Algorithm 4](#)) by keeping track of the remaining capacity at step k , defined by the following recursive equations:

$$s_0 = C,$$

$$s_k = \begin{cases} s_{k-1} - w_{i_k} & \text{if } i_k \in \mathcal{I}(\hat{x}), \\ s_{k-1} & \text{if } i_k \notin \mathcal{I}(\hat{x}), \end{cases} \quad \text{for } k = 1, \dots, n-1.$$

The nodes on the path are $p, (1, s_1), \dots, (n-1, s_{n-1}), q$. Applying [Algorithm 4](#) to the KPP instance in [Example 2](#) with 2 sampled solutions $\{1, 2, 3\}$ and $\{3, 4\}$, we have the initial decision diagram drawn in [Figure 5](#) (consider only solid and dashed arcs).

We define the set of valid transitions \mathcal{B} for the KPP to be:

$$\mathcal{B} = \left\{ b \left| \begin{array}{l} u(b) = (j, s_j) \in \mathcal{V}_j, \quad j = 0, \dots, n-1; \\ w(b) = (k, s_k) \in \mathcal{V}_k, \quad k = j+1, \dots, n; \\ s_j - \sum_{i \in I(b)} w_i \geq s_k \end{array} \right. \right\}.$$

In other words, a transition b from (j, s_j) to (k, s_k) is valid if and only if all items in $I(b)$ can be fit in a knapsack with capacity $s_j - s_k$. Recall that p and

q can be expressed as $(0, C)$ and $(n, 0)$. It is evident that given $u(b)$, $w(b)$, and $I(b)$, this condition can be tested efficiently. If we follow [Algorithm 5](#) and add the paths corresponding to $\{1, 4\}$ and $\{2, 4\}$, we will obtain the dotted arcs in [Figure 5](#).

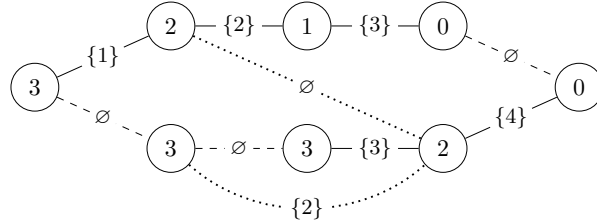


Figure 5: Dynamically generated decision diagram of [Example 7](#). Solid and dashed arcs are the initial arcs obtained from [Figure 4b](#), while dotted arcs are valid transitions added during [Algorithm 5](#). The labels of the nodes are the states s_k . The labels of the arcs are $I(a)$.

3.2.2 Item Grouping

A major disadvantage of decision diagrams compared to selection diagrams is the lack of scalability. For every new item, we need to add a whole new layer to the decision diagram, while the number of layers in a selection diagram stays at 4. Furthermore, many nodes just repeat the states of some nodes in the previous layers (see [Figure 4a](#)). In this section, we describe a technique to reduce the number of nodes in a decision diagram by grouping multiple items into one layer, instead of keeping the item-layer ratio at 1:1.

Let (J_1, \dots, J_m) be a list of disjoint subsets of \mathcal{I} such that $J_1 \cup \dots \cup J_m = \mathcal{I}$. We group all items in each *part* J_k together into 1 layer, so overall, the grouped decision diagram has $m + 1$ layers $\mathcal{V}_0, \mathcal{V}_1, \dots, \mathcal{V}_m$. For $k = 0, \dots, m - 1$, each node $u_k \in \mathcal{V}_k$ can have up to $2^{|J_{k+1}|}$ outgoing arcs towards the next layer \mathcal{V}_{k+1} . Each arc $a_{u_k}^K$ corresponds to a subset K of J_{k+1} with the item function simply defined as $I(a_{u_k}^K) = K$. Such an arc represents the decision of fixing $x_i = 1$ for all $i \in K$, and fixing $x_i = 0$ for all $i \in J_{k+1} \setminus K$. A path in the grouped diagram still represents a solution $\hat{x} \in \mathcal{X}$ because $\{J_1, \dots, J_m\}$ forms a partition of \mathcal{I} . Hence, all entries in x are fixed and no entry is fixed twice. [Algorithms 4](#) and [5](#) are extended accordingly.

Example 8. Consider the decision diagram in [Figure 4b](#). We group the first 2 layers into one group $J_1 = \{1, 2\}$ and the last 2 layers into another group $J_2 = \{3, 4\}$. The result is shown in [Figure 6a](#). The grouped version of [Figure 5](#) is illustrated in [Figure 6b](#).

In our experiments, we keep the number of layers m fixed and we partition the items randomly into groups of size $\lceil n/m \rceil$. This strategy allows us to maintain a constant number of nodes $|\hat{\mathcal{V}}|$ in the initial decision diagram as n

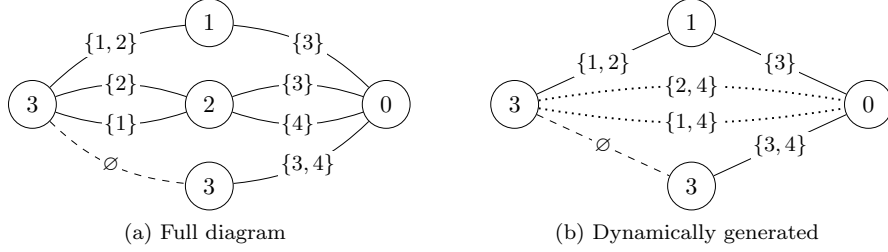


Figure 6: Grouped decision diagrams of [Example 8](#). Solid and dashed arcs are arcs in the initial diagram, dotted arcs are generated valid transitions. The labels of the nodes are the states s_k . The labels of the arcs are $I(a)$.

increases. We remark that this technique should be interpreted as a general framework, and one can develop new strategies depending on the situation, including groups with different sizes, subgroups inside a group, separate groups for tolled items and toll-free items, etc.

3.2.3 Maximum Stable Set Pricing Problem

We consider the case when the follower's problem is a maximum stable set problem. The overall pricing problem is called the *maximum stable set pricing problem* (MaxSSPP). Let $\mathcal{G} = (\mathcal{I}, \mathcal{E})$ be an undirected simple graph. In this case, the set of items \mathcal{I} is the set of nodes of \mathcal{G} . The objective of the follower is to find a *stable set* (*i.e.* a subset of \mathcal{I} in which no pair of nodes are adjacent) that maximizes the sum of tolled values. If $A \in \{0, 1\}^{\mathcal{I} \times \mathcal{E}}$ is the node-edge incidence matrix of \mathcal{G} , then the follower's problem of the MaxSSPP is formulated as follows:

$$\mathbf{R}(t) = \arg \max_x \{(v - t)^\top x \mid A^\top x \leq \mathbf{1}, x \in \{0, 1\}^{\mathcal{I}}\}$$

where $\mathbf{1}$ is the vector of all ones.

In the decision diagram for the MaxSSPP, the state s_k at step k is the set of all items in $\{i_{k+1}, \dots, i_n\}$ that are still available, *i.e.* they are not adjacent to any already-selected item. The arc $a_{u_k}^0$ is always available and it sends (k, s_k) to $(k + 1, s_k \setminus \{i_{k+1}\})$. The arc $a_{u_k}^1$ only exists if $i_{k+1} \in s_k$ (meaning the item i_{k+1} is available). In that case, it sends (k, s_k) to $(k + 1, s_k \setminus N[i_{k+1}])$ where $N[i]$ is the closed neighborhood of i (*i.e.* the set that includes i and all nodes adjacent to i). We express p as $(0, \mathcal{I})$ and q as (n, \emptyset) .

In regard to [Algorithm 4](#), given $\hat{x} \in \mathcal{X}$, we can generate a path corresponding to \hat{x} by the following recursive system:

$$s_0 = \mathcal{I},$$

$$s_k = \begin{cases} s_{k-1} \setminus N[i_k] & \text{if } i_k \in \mathcal{I}(\hat{x}), \\ s_{k-1} \setminus \{i_k\} & \text{if } i_k \notin \mathcal{I}(\hat{x}), \end{cases} \quad \text{for } k = 1, \dots, n.$$

The last piece is the definition of \mathcal{B} used in [Algorithm 5](#). A transition b from (j, s_j) to (k, s_k) is valid if and only if $I(b)$ is a stable set, $I(b) \subseteq s_j$, and $s_k \subseteq s_j \setminus N[I(b)]$.

Example 9. Consider a MaxSSPP instance of 5 items whose graph is shown in [Figure 7](#). Assuming that the item ordering is $(1, 2, 3, 4, 5)$, the initial decision diagram obtained from [Algorithm 4](#) with 2 sampled solutions $\{1, 3\}$ and $\{2, 5\}$ is drawn in [Figure 8](#) (consider only solid and dashed arcs). The dotted arcs in [Figure 8](#) represent the valid transitions generated by [Algorithm 5](#) corresponding to the 2 solutions $\{1, 4\}$ and $\{3, 5\}$.

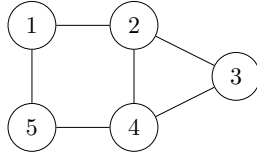


Figure 7: The graph \mathcal{G} of the MaxSSPP instance in [Example 9](#).

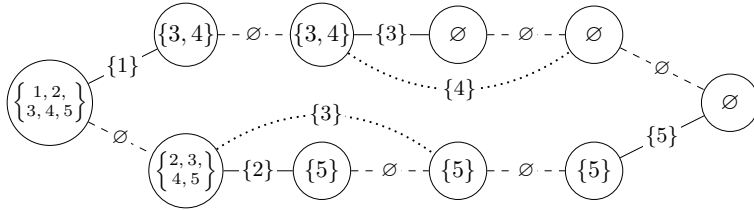


Figure 8: Dynamically generated decision diagram of [Example 9](#). Solid and dashed arcs are the initial arcs $a_{u_k}^1$ and $a_{u_k}^0$ respectively, while dotted arcs are generated valid transitions b . The labels of the nodes are the states s_k . The labels of the arcs are $I(a)$.

3.2.4 Minimum Set Cover Pricing Problem

The last pricing problem that we investigate is the *minimum set cover pricing problem* (MinSCPP), in which the follower solves a minimum set cover problem. Let \mathcal{E} be the set of elements that we wish to cover and let \mathcal{I} be a family of subsets of \mathcal{E} that covers \mathcal{E} (*i.e.* the union of all sets in \mathcal{I} is equal to \mathcal{E}). For the sake of consistency, we refer to subsets in \mathcal{I} as *items*. The follower aims to find a subset of \mathcal{I} that minimizes the sum of tolled values while still covering \mathcal{E} :

$$\mathbf{R}(t) = \arg \min_x \{(v + t)^\top x \mid Ax \geq \mathbf{1}, x \in \{0, 1\}^{\mathcal{I}}\}$$

where $A \in \{0, 1\}^{\mathcal{E} \times \mathcal{I}}$ is the incidence matrix between \mathcal{E} and \mathcal{I} . We make the assumption that the set of toll-free items \mathcal{I}_2 must cover \mathcal{E} , otherwise the leader can impose an infinite toll on all tolled items and the pricing problem is unbounded.

The state s_k in the MinSCPP is defined to be the set of uncovered elements of \mathcal{E} . In contrast to the first 2 problems, both arcs $a_{u_k}^0$ and $a_{u_k}^1$ are always available. The former sends (k, s_k) to $(k+1, s_k)$, and the latter sends (k, s_k) to $(k+1, s_k \setminus i_{k+1})$ (recall that i_{k+1} is a subset of \mathcal{E}). An exception exists in the next-to-last layer \mathcal{V}_{n-1} to check if the selected items form a cover: if $s_{n-1} \neq \emptyset$ (resp. $s_{n-1} \setminus i_n \neq \emptyset$), then the arc $u_{u_{n-1}}^0$ (resp. $u_{u_{n-1}}^1$) is not available. The nodes p and q are expressed as $(0, \mathcal{E})$ and (n, \emptyset) .

Given $\hat{x} \in \mathcal{X}$, a path corresponding to \hat{x} is generated using the recursive system:

$$s_0 = \mathcal{E},$$

$$s_k = \begin{cases} s_{k-1} \setminus i_k & \text{if } i_k \in \mathcal{I}(\hat{x}), \\ s_{k-1} & \text{if } i_k \notin \mathcal{I}(\hat{x}), \end{cases} \quad \text{for } k = 1, \dots, n.$$

Finally, a transition b from (j, s_j) to (k, s_k) is valid if and only if

$$s_j \setminus \left(\bigcup_{i \in I(b)} i \right) \subseteq s_k.$$

Example 10. Consider a MinSCPP instance where $\mathcal{E} = \{a, b, c, d\}$ and \mathcal{I} consists of 5 sets $i_1 = \{a, b\}$, $i_2 = \{a, c\}$, $i_3 = \{a, d\}$, $i_4 = \{b, c, d\}$, and $i_5 = \{c\}$. We order the items according to $(i_1, i_2, i_3, i_4, i_5)$. If we sample the solutions $\{i_1, i_3, i_5\}$ and $\{i_2, i_4\}$ for [Algorithm 4](#) and then generate valid transitions for $\{i_1, i_2, i_3\}$ and $\{i_3, i_4\}$ in [Algorithm 5](#), we will obtain the decision diagram illustrated in [Figure 9](#).

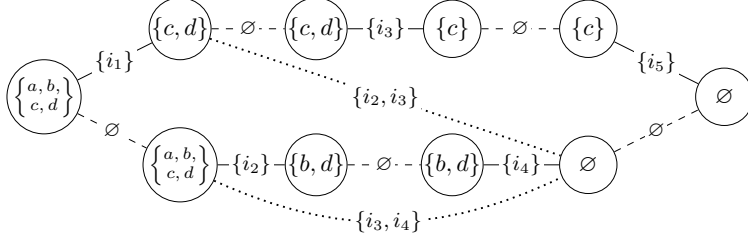


Figure 9: Dynamically generated decision diagram of [Example 10](#). Solid and dashed arcs are the initial arcs $a_{u_k}^1$ and $a_{u_k}^0$ respectively, while dotted arcs are generated valid transitions b . The labels of the nodes are the states s_k . The labels of the arcs are $I(a)$.

4 Experiments

We conducted numerical experiments to compare the performance of the 3 dynamic programming models: the value function reformulation (VF), the selection diagram (SD), and the decision diagram (DD). All 3 models were tested

on a family of randomly generated instances belonging to 3 pricing problems: the knapsack pricing problem (KPP), the maximum stable set pricing problem (MaxSSPP), and the minimum set cover pricing problem (MinSCPP). Additionally, we applied these models to a closely related problem that is the knapsack interdiction problem (KIP).

To evaluate the gradual impact of the selection diagram and the decision diagram compared to the control case (which is the value function reformulation), we vary the parameters N in Algorithm 2 and W in Algorithm 4. Note that if $N = 0$ and $W = 0$, then the programs corresponding to both diagrams become the value function reformulation. To reduce the variance when comparing the results with different values of N and W , we use the same random seed for all sampling procedures (lines 4, 5 in Algorithm 2, and line 4 in Algorithm 4). For the decision diagram, we also apply item grouping (Section 3.2.2) so that the number of layers is at most 20, except for the runs on the KPP where we group every 2 items together (since the numbers of items in the KPP instances are too low to be evenly divided into 20 layers).

Every run was executed on a single thread (AMD EPYC 7532 2.4GHz CPU, 8GB of RAM²) with the time limit of 1 hour. Mixed-integer programs are solved using Gurobi 9.5 [18] while the remaining code (formulation and constraint generation) are written in Julia 1.8.5. The dynamically generated constraints in Algorithms 1, 3 and 5 are implemented as lazy constraints in Gurobi. We reuse the bilevel feasible solutions (\hat{t}, \hat{x}) obtained during constraint generation as feasible solutions of the overall pricing problem. We supplement the solver with these solutions via a custom heuristic. Bounds for the McCormick envelope are provided in Appendix A. All instances and code are publicly available³.

The experimental results of each pricing problem are presented in Sections 4.1 to 4.3 respectively. In Section 4.4, we describe a modified formulation of Program (8) to apply our methodology to the KIP, followed by the corresponding experimental results. Finally, we provide a summary and our observations in Section 4.5.

4.1 Knapsack Pricing Problem

We generated random KPP instances that satisfy the following properties:

- The number of items $|Z|$ ranges from 40 to 60.
- The weights w_i are uniformly sampled in the range $[1, 100]$.
- The densities v_i/w_i are sampled uniformly in the range $[0.75, 1.25]$. The values v_i are then calculated by multiplying with the random weights.

²The experiment was run on the Narval computing cluster provided by the Digital Research Alliance of Canada.

³<https://github.com/minhcl95/CombinatorialPricing.jl>

- The proportion of tolled items $|\mathcal{I}_1|/|\mathcal{I}|$ is equal to the ratio between the capacity and the sum of weights, *i.e.* $C/\sum_{i \in \mathcal{I}} w_i$. We denote this proportion as r . Desirable values for r are from 0.5 to 0.6. The difficulty of the generated instances decreases sharply when r is outside of this range.
- The values v_i of the tolled items are multiplied by 2.0 afterward to encourage the use of tolled items. This technique is adopted from [6].

The parameters listed above are tuned using an evolutionary algorithm (CMA-ES [19]) to maximize the difficulty of the instances⁴. In total, 330 KPP instances were generated according to 33 different configurations (10 instances per configuration). These 33 configurations are the combinations of 11 values of $|\mathcal{I}| \in \{40, 42, \dots, 58, 60\}$, and 3 values of $r \in \{0.50, 0.55, 0.60\}$.

Table 1 shows the number of instances solved, the average time, and the average optimality gap of the 3 DP models with various values of N and W . The results of the best configurations of each model are plotted in Figures 10a and 10b. According to Table 1, the selection diagram does not improve the performance of the solution compared to the value function model, while the decision diagram does improve it slightly but only at low W (under 100). The knapsack problem is a relatively simple problem, containing only one constraint, so the time to solve the subproblem (included in the callback time) is negligible. The callback time increases when we increase the width W of the decision diagram, reflecting the fact that Algorithm 5 scales quadratically with respect to $|\hat{\mathcal{Y}}|$.

4.2 Maximum Stable Set Pricing Problem

Random MaxSSPP instances were generated on top of random graphs based on the Erdős-Rényi model. The parameters for the generation are as follows:

- The number of items $|\mathcal{I}|$ ranges from 120 to 180.
- The graph density, denoted as d , is from 0.12 to 0.24.
- The proportion of tolled items $|\mathcal{I}_1|/|\mathcal{I}|$ is 0.4.
- The values v_i are uniformly sampled in the range $[50, 150]$, then those of the tolled items are multiplied by 1.3.

Similar to the KPP instances, these parameters are tuned using the same evolutionary process. We generated 280 instances in total with respect to 28 configurations: 7 values of $|\mathcal{I}| \in \{120, 130, \dots, 180\}$ combined with 4 values of $d \in \{0.12, 0.16, 0.20, 0.24\}$.

Table 2 and Figure 10c show the results of the experiments on the MaxSSPP. The decision diagram still produces a slight improvement and its performance

⁴Evaluated via the difference between the null-toll value (when $t = 0$) and the toll-free value (when $t \rightarrow \infty$) of the follower’s problem. Larger difference means that the optimal solution is less trivial.

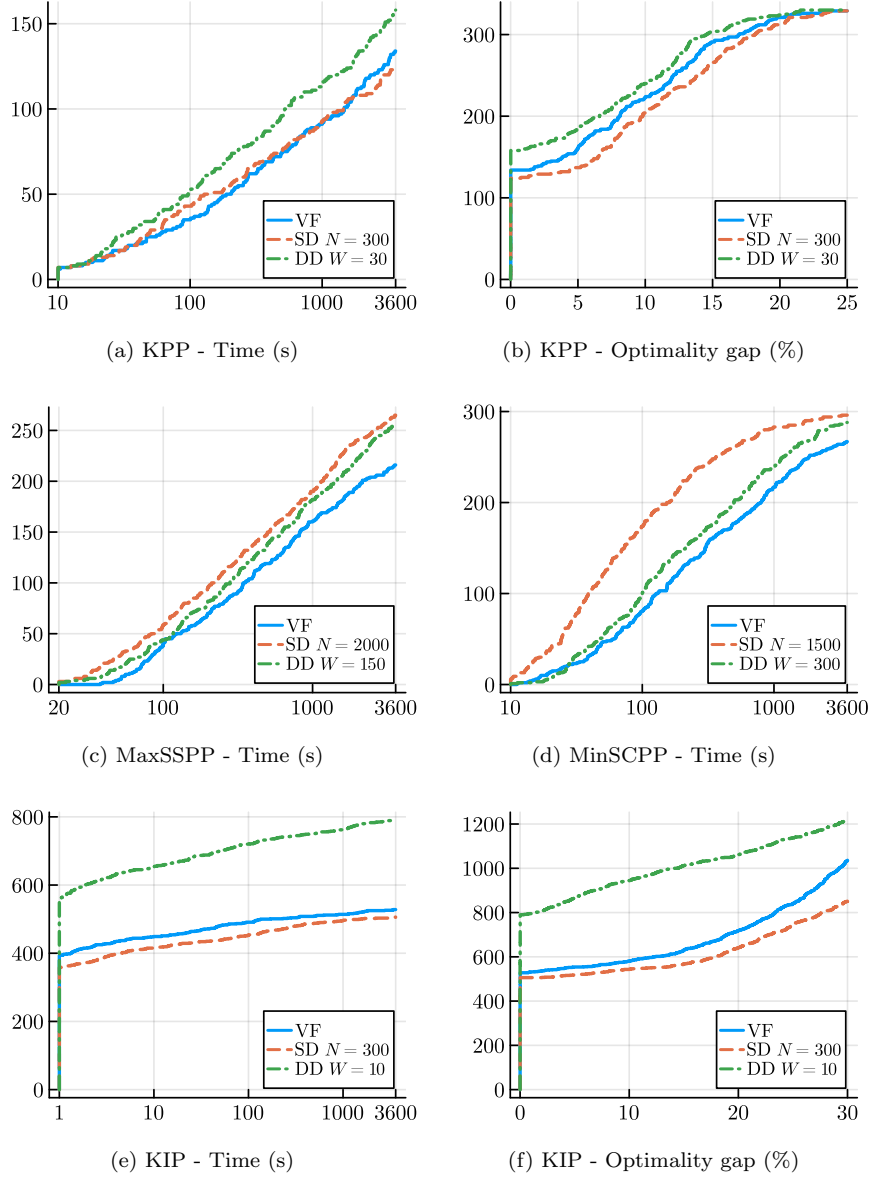


Figure 10: Cumulative number of instances (y -axis) with respect to solution time and optimality gap (x -axis). The time is depicted in logarithmic scale, while a linear scale is used for the gap.

Table 1: Numerical results for the KPP.

DP Model	N/W	Num. of instances solved	Time ^a (s)		Gap ^b (%)
			Total	Callback	
VF		134	1301	6	6.5
SD	100	118	1316	10	7.6
SD	200	121	1263	10	7.7
SD	300	124	1263	10	7.6
SD	500	120	1333	9	7.7
SD	700	117	1379	10	7.8
SD	1000	113	1402	10	8.1
SD	1500	118	1465	10	8.0
SD	2000	116	1431	10	7.9
SD	2500	113	1452	10	8.0
SD	3000	114	1487	11	8.2
DD	10	147	973	5	5.7
DD	20	157	994	5	5.5
DD	30	158	980	6	5.4
DD	50	150	1082	10	5.6
DD	70	144	1155	14	5.6
DD	100	135	1327	19	6.0
DD	150	124	1540	30	6.6
DD	200	113	1735	42	7.1
DD	250	106	1923	53	7.5
DD	300	100	2070	64	7.9

^a Geometric average.

^b Arithmetic average.

The best configuration of each model is highlighted in bold.

Table 2: Numerical results for the MaxSSPP.

DP Model	N/W	Num. of instances solved	Time ^a (s)		Gap ^b (%)	Num. of callback calls ^a	Time per callback call ^a (s)
			Total	Callback			
VF		216	654	650	15.0	202	3.22
SD	100	230	655	650	10.0	201	3.24
SD	200	228	611	606	10.8	194	3.12
SD	300	234	610	604	10.6	202	3.00
SD	500	252	500	493	4.9	191	2.58
SD	700	250	457	449	3.8	185	2.42
SD	1000	257	415	407	3.7	181	2.25
SD	1500	254	393	384	4.3	174	2.20
SD	2000	265	389	379	2.0	172	2.21
SD	2500	261	381	371	2.6	168	2.20
SD	3000	259	387	375	2.9	167	2.25
DD	10	251	543	537	4.9	192	2.80
DD	20	247	496	489	4.4	184	2.65
DD	30	250	493	486	4.2	188	2.58
DD	50	252	502	493	4.0	189	2.61
DD	70	255	483	474	4.2	181	2.62
DD	100	253	484	473	4.1	186	2.54
DD	150	257	487	473	3.4	181	2.61
DD	200	254	499	481	5.1	176	2.73
DD	250	258	509	487	3.7	175	2.78
DD	300	254	478	456	4.9	169	2.70

^a Geometric average.

^b Arithmetic average.

The best configuration of each model is highlighted in bold.

is less sensitive to W . In contrast to the KPP, the selection diagram at high N surpasses the decision diagram. At $N = 2000$, the selection diagram model can solve 50 more instances and is more than 1.5 times faster compared to the value function model. Unlike the KPP, the callback time (which includes the time to solve the subproblem) dominates the total solution time. Thus, both diagrams benefit from the decreases in the number of callback calls and the time per callback call.

4.3 Minimum Set Cover Pricing Problem

The generation of MinSCPP instances is more complex compared to the other 2 problems. First, every element $e \in \mathcal{E}$ is given its own value w_e sampled uniformly in $[50, 85]$. Then, we synthesize the sets $i \in \mathcal{I}$ by including each element in \mathcal{E} with probability 0.23. Special care is required to ensure \mathcal{I} covers \mathcal{E} . The value v_i is calculated as the sum of w_e for all $e \in i$, then it is perturbed by a factor sampled within $[0.9, 1.1]$. Next, we find a subcover of \mathcal{I} to form the set of toll-free items \mathcal{I}_2 (recall that \mathcal{I}_2 must cover \mathcal{E} otherwise the leader can impose an infinite toll). The proportion of tolled items is 0.3. Finally, the values of the tolled items are divided by 2.3. All parameters are tuned using an evolutionary algorithm.

We experimented with 6 values of $|\mathcal{I}| \in \{70, 80, \dots, 120\}$ and 5 values of $|\mathcal{I}|/|\mathcal{E}| \in \{0.8, 1.0, 1.2, 1.4, 1.6\}$, combined to create 30 configurations, hence 300 random MinSCPP instances.

The results for the MinSCPP are displayed in [Table 3](#) and [Figure 10d](#). Similar to the MaxSSPP, the callback time plays a major role in the total solution time. The selection diagram greatly outperforms the other 2 models. At $N = 1500$, it can solve almost all instances and is 3.5 times faster than the value function model. The main contribution is the drop in the number of callback calls by 3 times. It also reduces the time spent per callback call by 20%.

4.4 Knapsack Interdiction Problem

The KIP proposed by [\[12\]](#) is not strictly a pricing problem. Nevertheless, we can utilize the same methodology to derive a single-level reformulation similar to [Program \(8\)](#). For the sake of consistency, let $t, x \in \{0, 1\}^{\mathcal{I}}$ denote the leader's decision and the follower's decision, respectively. Then, the KIP has the following bilevel formulation:

$$\min_t \{f(t) \mid W^\top t \leq C, t \in \{0, 1\}^{\mathcal{I}}\}$$

where $f(t)$ is the optimal objective value of the integer program:

$$f(t) = \max_x \{v^\top x \mid w^\top x \leq c, x \leq 1 - t, x \in \{0, 1\}^{\mathcal{I}}\}. \quad (9)$$

Due to [Caprara et al. \[9\]](#), we can rewrite [Program \(9\)](#) as:

$$f(t) = \max_x \left\{ \sum_{i \in \mathcal{I}} (v_i - v_i t_i) x_i \mid w^\top x \leq c, x \in \{0, 1\}^{\mathcal{I}} \right\}. \quad (10)$$

Table 3: Numerical results for the MinSCPP.

DP Model	N/W	Num. of instances solved	Time ^a (s)		Gap ^b (%)	Num. of callback calls ^a	Time per callback call ^a (s)
			Total	Callback			
VF		267	313	302	10.1	305	0.99
SD	100	282	259	248	7.3	282	0.88
SD	200	283	251	240	6.5	273	0.88
SD	300	283	210	199	5.8	238	0.84
SD	500	283	130	120	3.8	145	0.83
SD	700	292	94	84	1.0	107	0.79
SD	1000	294	88	79	0.4	99	0.80
SD	1500	296	89	80	0.4	100	0.80
SD	2000	293	99	89	0.3	110	0.80
SD	2500	292	110	99	0.5	120	0.82
SD	3000	295	129	116	0.3	141	0.82
DD	50	282	244	231	7.1	264	0.88
DD	100	283	232	216	5.3	255	0.85
DD	150	280	227	208	5.7	244	0.85
DD	200	284	228	205	5.4	241	0.85
DD	250	284	221	196	5.0	226	0.87
DD	300	288	230	203	3.5	224	0.91

^a Geometric average.

^b Arithmetic average.

The best configuration of each model is highlighted in bold.

We observe that [Program \(10\)](#) has the same form as [Program \(1\)](#). As a result, we can replace [Program \(10\)](#) with a DP model as in [Program \(7\)](#). The overall single-level reformulation of the KIP is:

$$\min_{t,x,y} y_p \tag{11a}$$

$$\text{s.t. } W^\top t \leq C, \tag{11b}$$

$$w^\top x \leq c, \tag{11c}$$

$$y_{u(a)} \geq F(a; t) + y_{w(a)}, \quad a \in \mathcal{A}, \tag{11d}$$

$$y_q = 0, \tag{11e}$$

$$t, x \in \{0, 1\}^{\mathcal{I}}. \tag{11f}$$

Note that the realization of [Constraints \(11d\)](#) and [\(11e\)](#) depends on the chosen DP model (whether it is the value function, selection diagram, or decision diagram). Moreover, we reuse y_p in [\(11a\)](#), since both the leader and the follower in the KIP optimize the same objective function but in opposite directions. As a side effect, [Program \(11\)](#) is free from bilinear terms (contrary to the reformulation of [\[22\]](#)) and hence, it does not require linearization (as described in [Section 2.2](#)).

We tested the 3 DP models on the set of 1340 instances mentioned in [\[28\]](#). In particular, the instances are taken from CCLW [\[9\]](#), DCS [\[11\]](#), DeNegre [\[12\]](#), FMS [\[16\]](#), and TRS [\[27\]](#). However, we exclude the 1500 newly-generated instances in [\[28\]](#) because they have a very high number of items and our approaches are unable to solve them; we recall that our framework is aimed to be general-purpose. The results are shown in [Table 4](#) and [Figures 10e](#) and [10f](#). The decision diagram is clearly superior than the other 2 models in every class of instances. Comparing the DP models to the state of the art method described in [\[28\]](#), our models are worse, but our experiments are executed on a single thread, while theirs were run using 16 threads. Nonetheless, the DP models are more general and should not be expected to outperform problem-specific algorithms. Analogously, the branch-and-bound method by [\[16\]](#) for interdiction problems with monotonicity (recall [Remark 2](#)) is overall faster than our models, for the instances they tested: CCLW, TRS and part of DeNegre. Despite this, our decision diagram model with $W = 10$ solved all those instances in much less time than the time limit and it was significantly faster than the running times reported for the general bilevel solver MIX++ in [\[15\]](#).

4.5 Discussions

The experiments on 4 different problems give us a well-rounded view on the effectiveness of the diagram models. The decision diagram is robust and can provide a small boost in any circumstance compared to the value function reformulation. The selection diagram, however, only performs well in the MaxSSPP and the MinSCPP. The central mechanism of the improvement is due to the reductions in the number of callback calls and the time spent per call. In

Table 4: Numerical results for the KIP.

DP Model	N/W	Num. of instances solved	Time ^a (s)						Gap ^b (%)
			Total	CCLW	DCS	DeNegre	FMS	TRS	
VF	0	528	197	10	2415	3	574	1	16
SD	100	497	236	18	2477	5	785	1	18
SD	200	500	238	19	2421	5	799	1	18
SD	300	506	239	22	2390	5	789	1	18
SD	500	504	244	22	2454	6	788	1	18
SD	700	506	245	27	2444	6	784	1	18
SD	1000	501	252	29	2519	6	795	1	18
SD	1500	503	252	27	2556	6	794	1	18
SD	2000	502	255	28	2595	6	797	1	18
SD	2500	500	257	30	2643	6	790	1	18
SD	3000	503	258	29	2641	6	803	1	18
DD	10	790	51	2	346	1	154	1	8
DD	20	786	54	2	378	1	168	1	8
DD	30	783	56	3	398	1	170	1	8
DD	50	780	59	3	423	1	177	1	9
DD	70	770	62	3	443	1	184	1	9
DD	100	763	64	3	458	2	187	1	9
DD	150	759	66	4	469	2	187	1	9
DD	200	756	68	4	482	2	184	1	9
DD	250	751	69	5	483	2	184	1	9
DD	300	741	70	5	477	2	181	1	9

^a Geometric average. Values less than 1 are lifted to 1.

^b Arithmetic average.

The best configuration of each model is highlighted in bold.

particular, most of the solution time is spent to solve the subproblem in the MaxSSPP and MinSCPP, while for the KPP and the KIP, that time is spent mainly on branch-and-bound.

We remark the dissimilarities in the structures of the 4 problems. In the KPP and the KIP, any pair of items can appear in a feasible solution (as long as C is large enough). This is not the case for the MaxSSPP, whose main constraint is the exclusion of certain pairs of items. In the MinSCPP, although any pair can also appear in a feasible solution, the minimality of a cover discourages the selection of pair of items that have many overlaps in \mathcal{E} . Furthermore, a maximal solution of the KPP contains around 50% of all items. This number is smaller in the other 2 problems: 20% for the MaxSSPP and 10% for the MinSCPP. The disparity in the distribution of pairs in feasible solutions may explain the unevenness in the performance of the selection diagram across the 3 problems.

5 Conclusion

In this paper, we derived a single-level reformulation of the CPP by taking the dual of a linear program corresponding to a dynamic programming model of the follower’s problem, and combining it with the original primal problem using strong duality. We investigated 2 dynamic programming models: selection diagram and decision diagram, and provided the algorithms to solve them dynamically. Then, we tested these models in 3 specializations of the CPP as well as the KIP. We observed that the decision diagram model can consistently lead to performance improvements over the value function reformulation, while the selection diagram formulation only brings (significant) speedups for 2 specializations of the CPP.

Future research directions include the exploration of other dynamic programming models and the application of this technique to other problems in bilevel optimization.

A Bounds for the McCormick envelope

To solve [Program \(8\)](#) as a MILP, one needs to linearize the bilinear terms $t^\top x$ using the McCormick envelope ([Equation \(6\)](#)). As explained in [Section 2.2](#), $M_i = v_i$ is a valid bound for the KPP due to [Remark 1](#). By a similar reasoning, $M_i = v_i$ is still a valid bound for the MaxSSPP. However, this logic crumbles in the case of the MinSCPP because of the optimization direction.

To derive a valid bound for the MinSCPP, we take inspiration from the same linearization problem occurring in the NPP [[13](#)]. Recall that in the MinSCPP, each $i \in \mathcal{I}$ is a subset of \mathcal{E} (see [Section 3.2.4](#)). For $i \in \mathcal{I}$, a valid bound M_i for $t_i x_i$ is:

$$\max\{0, \min\{P_i, Q_i\}\}$$

where

$$\begin{aligned} P_i &= f(\infty; i) - v_i, \\ Q_i &= f(\infty; \mathcal{E}) - f(0; \mathcal{E} \setminus i) - v_i. \end{aligned}$$

The function $f(t; E)$ is defined to be the total cost to cover all elements in $E \subseteq \mathcal{E}$ given tolls t :

$$f(t; E) = \min_x \{(v + t)^\top x \mid A_E x \geq \mathbf{1}, x \in \{0, 1\}^{\mathcal{I}}\}$$

where $A_E \in \{0, 1\}^{E \times \mathcal{I}}$ is the incidence matrix between E and \mathcal{I} . In particular, $f(\infty; E)$ is the cost to cover E without using any tolled set in \mathcal{I}_1 (also called the *toll-free cost*), while $f(0; E)$ is the cost to cover E when all tolled sets are available for no extra costs (also called the *null-toll cost*).

The bound P_i is valid because if $t_i > P_i$, then we can replace the set i with the toll-free sets in the optimal solution of $f(\infty; i) < v_i + t_i$, which still cover all elements in i but with less total cost.

The bound Q_i is valid because the lowest cost for any solution that includes i is $f(0; \mathcal{E} \setminus i) + v_i + t_i$. If $t_i > Q_i$, then the toll-free solution of $f(\infty; \mathcal{E})$ will have lower cost than any solution that contains i , meaning the latter can never be optimal when $t_i > Q_i$.

Acknowledgments

This work was funded by FRQ-IVADO Research Chair in Data Science for Combinatorial Game Theory, and the NSERC grant 2019-04557.

This research was enabled in part by support provided by Calcul Québec (<https://www.calculquebec.ca>) and the Digital Research Alliance of Canada (<https://alliancecan.ca>).

References

- [1] David Bergman, Andre A. Cire, Willem-Jan van Hoeve, and J. N. Hooker. Discrete optimization with decision diagrams. *INFORMS Journal on Computing*, 28(1):47–66, 2016. doi: 10.1287/ijoc.2015.0648.
- [2] Dimitri Bertsekas. *Dynamic programming and optimal control: Volume I*, volume 4. Athena scientific, 2012.
- [3] Mustapha Bouhtou, Stan van Hoesel, Anton F. van der Kraaij, and Jean-Luc Lutton. Tariff optimization in networks. *INFORMS Journal on Computing*, 19(3):458–469, 2007. doi: 10.1287/ijoc.1060.0177.
- [4] Patrick Briest, Luciano Gualà, Martin Hoefer, and Carmine Ventre. On Stackelberg pricing with computationally bounded customers. *Networks*, 60(1):31–44, 2012. doi: 10.1002/net.20457.

- [5] Patrick Briest, Martin Hoefer, and Piotr Krysta. Stackelberg network pricing games. *Algorithmica*, 62(3-4):733–753, 2012. doi: 10.1007/s00453-010-9480-3.
- [6] Luce Brotcorne, Martine Labbé, Patrice Marcotte, and Gilles Savard. A bilevel model and solution algorithm for a freight tariff-setting problem. *Transportation Science*, 34(3):289–302, 2000. doi: 10.1287/trsc.34.3.289.12299.
- [7] Quang Minh Bui, Bernard Gendron, and Margarida Carvalho. A catalog of formulations for the network pricing problem. *INFORMS Journal on Computing*, 34(5):2658–2674, 2022. doi: 10.1287/ijoc.2022.1198.
- [8] Toni Böhnlein, Oliver Schaudt, and Joachim Schauer. Stackelberg packing games. *Theoretical Computer Science*, 943:16–35, 2023. ISSN 0304-3975. doi: 10.1016/j.tcs.2022.12.006.
- [9] Alberto Caprara, Margarida Carvalho, Andrea Lodi, and Gerhard J Woeginger. Bilevel knapsack with interdiction constraints. *INFORMS Journal on Computing*, 28(2):319–333, 2016. doi: 10.1287/ijoc.2015.0676.
- [10] Jean Cardinal, Erik D Demaine, Samuel Fiorini, Gwenaél Joret, Stefan Langerman, Ilan Newman, and Oren Weimann. The Stackelberg minimum spanning tree game. *Algorithmica*, 59:129–144, 2011. doi: 10.1007/s00453-009-9299-y.
- [11] Federico Della Croce and Rosario Scatamacchia. An exact approach for the bilevel knapsack problem with interdiction constraints and extensions. *Mathematical Programming*, 183(1-2):249–281, 2020. doi: 10.1007/s10107-020-01482-5.
- [12] Scott DeNegre. *Interdiction and discrete bilevel linear programming*. PhD thesis, Lehigh University, 2011.
- [13] Sophie Dewez, Martine Labbé, Patrice Marcotte, and Gilles Savard. New formulations and valid inequalities for a bilevel pricing problem. *Operations Research Letters*, 36(2):141–149, 2008. ISSN 0167-6377. doi: 10.1016/j.orl.2007.03.005.
- [14] Mohamed Didi-Biha, Patrice Marcotte, and Gilles Savard. Path-based formulations of a bilevel toll setting problem. In *Optimization with Multivalued Mappings: Theory, Applications, and Algorithms*, pages 29–50. Springer US, 2006. doi: 10.1007/0-387-34221-4_2.
- [15] Matteo Fischetti, Ivana Ljubić, Michele Monaci, and Markus Sinnl. A new general-purpose algorithm for mixed-integer bilevel linear programs. *Operations Research*, 65(6):1615–1637, 2017. doi: 10.1287/opre.2017.1650.

- [16] Matteo Fischetti, Michele Monaci, and Markus Sinnl. A dynamic reformulation heuristic for generalized interdiction problems. *European Journal of Operational Research*, 267(1):40–51, 2018. doi: 10.1016/j.ejor.2017.11.043.
- [17] Matteo Fischetti, Ivana Ljubić, Michele Monaci, and Markus Sinnl. Interdiction games and monotonicity, with application to knapsack problems. *INFORMS Journal on Computing*, 31(2):390–410, 2019. doi: 10.1287/ijoc.2018.0831.
- [18] Gurobi Optimization, LLC. Gurobi Optimizer Reference Manual, 2022. URL <https://www.gurobi.com>.
- [19] Nikolaus Hansen, Sibylle D Müller, and Petros Koumoutsakos. Reducing the time complexity of the derandomized evolution strategy with covariance matrix adaptation (CMA-ES). *Evolutionary computation*, 11(1):1–18, 2003. doi: 10.1162/106365603321828970.
- [20] Géraldine Heilporn, Martine Labbé, Patrice Marcotte, and Gilles Savard. New formulations and valid inequalities for the toll setting problem. *IFAC Proceedings Volumes*, 39(3):431–436, 2006. ISSN 1474-6670. doi: 10.3182/20060517-3-FR-2903.00228. 12th IFAC Symposium on Information Control Problems in Manufacturing.
- [21] Martine Labbé, Patrice Marcotte, and Gilles Savard. A bilevel model of taxation and its application to optimal highway pricing. *Management Science*, 44(12-part-1):1608–1622, 1998. doi: 10.1287/mnsc.44.12.1608.
- [22] Leonardo Lozano, David Bergman, and Andre A Cire. Constrained shortest-path reformulations for discrete bilevel and robust optimization. *arXiv preprint arXiv:2206.12962*, 2022. doi: 10.48550/arXiv.2206.12962.
- [23] Garth P McCormick. Computability of global solutions to factorable non-convex programs: Part i—convex underestimating problems. *Mathematical programming*, 10(1):147–175, 1976. doi: 10.1007/BF01580665.
- [24] Ulrich Pferschy, Gaia Nicosia, Andrea Pacifici, and Joachim Schauer. On the Stackelberg knapsack game. *European Journal of Operational Research*, 291(1):18–31, 2021. ISSN 0377-2217. doi: 10.1016/j.ejor.2020.09.007.
- [25] Sébastien Roch, Gilles Savard, and Patrice Marcotte. An approximation algorithm for Stackelberg network pricing. *Networks*, 46(1):57–67, 2005. doi: 10.1002/net.20074.
- [26] Sahar Tahernejad, Ted K Ralphs, and Scott T DeNegre. A branch-and-cut algorithm for mixed integer bilevel linear optimization problems and its implementation. *Mathematical Programming Computation*, 12:529–568, 2020. doi: 10.1007/s12532-020-00183-6.

- [27] Yen Tang, Jean-Philippe P Richard, and J Cole Smith. A class of algorithms for mixed-integer bilevel min–max optimization. *Journal of Global Optimization*, 66:225–262, 2016. doi: 10.1007/s10898-015-0274-7.
- [28] Noah Weninger and Ricardo Fukasawa. A fast combinatorial algorithm for the bilevel knapsack problem with interdiction constraints. In *Integer Programming and Combinatorial Optimization*, pages 438–452, Cham, 2023. Springer International Publishing. ISBN 978-3-031-32726-1. doi: 10.1007/978-3-031-32726-1_31.